Available online at www.sciencedirect.com
ScienceDirect
Electrochimica Acta 53 (2007) 324–329
ELECTROCHIMICA Acta
www.elsevier.com/locate/electacta

Copper nanowires and silver micropit arrays from the electrochemical treatment of a directionally solidified silver–copper eutectic

Sarah Brittman [a,b], Andrew Jonathan Smith [a], Srdjan Milenkovic [a], Achim Walter Hassel [a,*,1]

[a] *Max-Planck-Institut für Eisenforschung, Max-Planck-Str. 1, 40237 Düsseldorf, Germany*
[b] *Harvard University, Cambridge, MA 02138, USA*

Received 9 March 2007; received in revised form 8 June 2007; accepted 13 July 2007
Available online 28 July 2007

Abstract

The method of fabricating metallic nanowires from directionally solidified eutectics was applied to the silver–copper system. The silver–copper alloy, 39.9 at.% copper, was directionally solidified in a Bridgman-type oven held at 850 °C. SEM imaging revealed a mixed fibrous and lamellar microstructure. The fastest solidification rates produced fibres and lamellae with widths as small as 300 nm. Electrochemical conditions for the selective dissolution of silver and of copper were determined from the combined Pourbaix diagram for silver and copper and applied to the directionally solidified alloy. Subsequent microscopic investigations yielded copper nanowires with diameters in the 300–640 nm range and hexagonal arrays of micropits in the silver matrix with diameters of 1 μm. The chosen volume fraction of the Ag–Cu system is the only one that matches exactly the theoretical value of π^{-1} which separates fibrous from lamellar structures. It is demonstrated that the simultaneous formation of fibres and lamellae in the same sample occurs for this unique borderline system.

Keywords: Directional solidification; Silver–copper eutectic; Copper Nanowires; Micropit

1. Introduction

Cu–Ag alloys with filamentary structure of double phases are widely studied for their outstanding strength and conductivity [1–3]. After heavy cold drawing, materials with excellent properties could be obtained. The nanoscale structure evolved from the original eutectic colonies consists of secondary precipitates and primary α grains [4–9]. These materials are expected to be used primarily in the magnetic windings of high field magnets, where high mechanical strength and excellent electrical conductivity are required to withstand the Lorentz force and minimize the Joule heating produced by the strong electrical current [10–12]. The attractive properties of a tensile strength exceeding 1 GPa with a conductivity of (60–70)% International Annealed Copper Standard (IACS) has been realized in Cu–Ag microcomposites, and further improvements are still expected through the development and design of high field magnets [5,13,14]. Furthermore, Ag–Cu binary and Al–Ag–Cu ternary systems have often been selected as model systems for studying the formation of the so-called banded structure in rapidly solidified alloys and their nucleation [15], microstructure formation, and pattern selection along a ternary eutectic solidification path [16–19]. Also, a Sn–Ag–Cu ternary eutectic is considered the best candidate for lead-free solders to replace Sn–Pb solders as low temperature joining alloys in the electronic packaging industries [20–23]. For a system with such promising applications, however, studies considering the directional solidification of Ag–Cu binary alloys are rather scarce. The most detailed work comes from Frommeyer et al., who analysed the microstructure and properties of directionally solidified and cold drawn Ag–Cu eutectics [4,24]. No information exists, however, on the production of ordered micro- or nanostructures from this system. Recently a method was developed for making various nano-structures from directionally solidified eutectics [25–29]. It combines directional solidification of eutectic alloys to produce self-organised nano-structures and selective etching and/or electrochemical dissolution to separate

* Corresponding author. Fax: +49 211 6792 218.
E-mail address: hassel@elchem.de (A.W. Hassel).
[1] ISE active member.

0013-4686/$ – see front matter © 2007 Elsevier Ltd. All rights reserved.
doi:10.1016/j.electacta.2007.07.048

the phases. In this study, this novel method was applied to the Ag–Cu system.

2. Experimental

Pre-alloys were prepared from silver (99.99 wt.%) and electrolytic copper (99.99 wt.%) by induction melting under an inert atmosphere and drop casting into a cylindrical copper mould. Subsequently, ingots of the eutectic alloy were enclosed in evacuated quartz vials. A vial was suspended within the channel of a cylindrical furnace heated to 850 ± 5 °C and the alloy allowed to melt. A motor lowered the vial at a constant rate through the furnace and into a glass funnel at its base (Fig. 1). The motor used was manufactured by Faulhaber (Schönaich, Germany) running at a maximum of 14,400 rpm combined with 1:235,067 ultra low translation gears in order to realize constant and slow movement. This movement from the heat of the furnace into the funnel provided the temperature gradient necessary for directional solidification. The glass funnel reduced air currents within the furnace's channel, which stabilized its temperature. Rates of 53 mm h^{-1} (14.7 μm s^{-1}), 91 mm h^{-1} (25 μm s^{-1}) and 245 mm h^{-1} (68.1 μm s^{-1}) were investigated.

Samples for further investigations were cut from the *ds*-ingot horizontally to the growth direction to allow a top view into the structure. After standard mechanical grinding with subsequently finer emery papers, the directionally solidified samples were treated electrochemically to selectively dissolve either the silver matrix or the copper wires. The copper phase was dissolved by exposing the sample to 1.0 M acetate buffer (pH 6.0), and applying a potential of 0.5 V (SHE). In order to selectively dissolve the silver phase the samples were polarized to 0.7 V (SHE) in 0.1 M borate buffer (pH 9.2). The strategies used for this selective dissolution are discussed in detail in the results section.

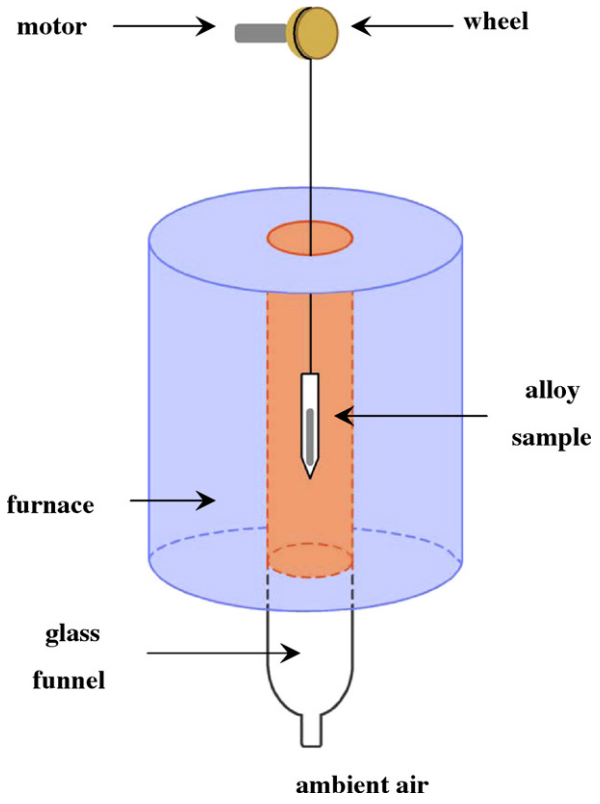

Fig. 1. Schematic of the directional solidification setup.

Polarization of the samples was performed with an EG&G Princeton Applied Research 287 potentiostat in a standard three-electrode cell with working, counter, and reference electrodes. A Ag/AgCl electrode was used as a reference. Noticeable dissolution of the copper fibres took only a few hours, while dissolution of the silver matrix occurred much more slowly. After electrochemical treatment, samples were ultrasonicated in deionised water to remove surface particles. For samples subjected to dissolution of the silver matrix, ultrasonication removed the insoluble copper oxide layer, which could be seen as a reddish-brown powder deposited in the water.

Samples were imaged with a field emission scanning electron microscope (Zeiss LEO 1550VP) using both in-lens and secondary electron detectors. All chemicals were p.a. grade and obtained from VWR International GmbH, Darmstadt, Germany.

3. Results and discussion

3.1. The eutectic point

The Ag–Cu phase diagram has been extensively studied. The liquidus curve was first published by Roberts–Austen as early as 1875 [30], and the existence of a eutectic was recognized by the same author in 1891 [31]. The eutectic temperature has been reported in the range from 777 to 780 °C [32–36]. Hansen [37] accepted a value of 779.8 °C from Roesner [34]. More recent thermal analysis by Moser et al. [36] using high-purity materials placed the eutectic temperature at 779.1 ± 0.08 °C. This value has been favoured in the review by Hansen and Elliot [38]. The composition values for the eutectic have been reported in a narrow range between 39.8 and 41.0 at.% Cu [33,35,39]. The value of 39.9 at.% Cu selected in this study has an uncertainty of less than 0.2 at.% [37]. The composition of the Ag–Cu alloy used was confirmed by chemical analysis using ICP-OES (inductively coupled plasma optical emission spectrometry).

3.2. Lamellar versus fibrous growth

The directional solidification of silver–copper eutectics produced a mixture of fibrous and lamellar microstructures. According to the theory of crystal growth [40], the morphology of the eutectic structure depends upon the volume fractions of the eutectic phases. At high volume fractions V_f of both phases ($V_f > \pi^{-1} \approx 0.318$) there is a marked preference for the formation of lamellar structures. On the other hand, if one phase is present in a small volume fraction ($V_f < \pi^{-1} \approx 0.318$), there is a strong tendency to form fibres of that phase. Applying the lever rule, volume fractions of the phases for the Ag–Cu eutectic are calculated to be 31.8 vol.% of Cu and 62.1 vol.% of Ag. Among all systems the Ag–Cu system matches best the theoretical value of π^{-1}. The fact that contiguous grains in directionally solidified alloys often show quite different morphologies is an important

observation related to the orientation relationships, the implications of which are often insufficiently considered. A plausible explanation for the observed difference in morphology is that the orientation relationships between the phases are different in the two grains. According to Hunt and Chilton [41] the preferential morphology is the one that grows with the least undercooling. In an approximate calculation they showed that the undercooling for fibres is less than that for lamellae when the volume fraction of the fibrous phase (V_f) is

$$V_f < \pi \left(\frac{\sigma_L}{\sigma_F} \right)^2 \quad (1)$$

where σ_L is the interphase energy per unit area between the lamellae, and σ_F is the interphase energy per unit area around the fibres. In the case of interphase energy anisotropy and volume fractions near the critical one, σ_L may be small enough – for some crystallographic orientations and growth directions – for lamellae to be formed, but for other conditions σ_L approaches σ_F, and therefore fibres are formed.

3.3. Quantitative evaluation of the microstructure

Some cells of the samples evidenced a regular hexagonal arrangement of copper fibres within the silver matrix and an example of which is shown in Fig. 2. The copper appears darker than the silver in this SEM image. The hexagonal pattern is often observed in self-organizing systems under diffusion control, e.g. in the formation of porous anodic aluminium. The initial copper wires try to achieve a circular cross-section in order to minimise their surface energy, and at the same time they are competing with each other to collect the copper atoms from the undercooled zone. Thus they tend to minimise the interfibre distance for this diffusion-controlled process. The densest packing of circles in a plane is a hexagonal packing. A quantitative measure of how closely this ideal structure has been achieved can be derived from the distribution function of the number of nearest neighbours for each fibre. This figure was analyzed by converting it to a binary image and using a MATLAB script to sum up the pixels

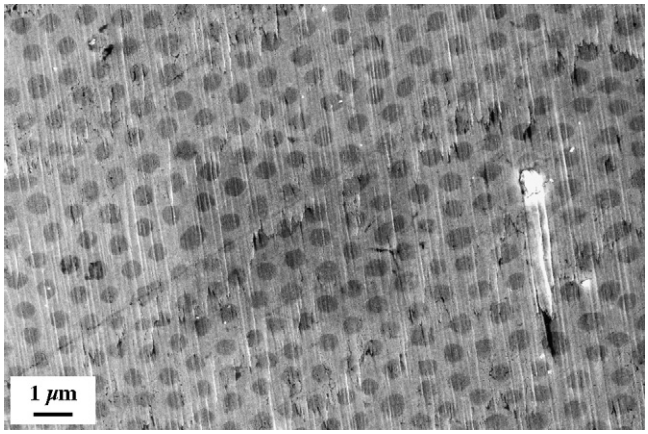

Fig. 2. SEM image of the polished cross-section of the directionally solidified eutectic. The dark circles are the cross-sections of the copper fibres that are embedded in the lighter silver matrix.

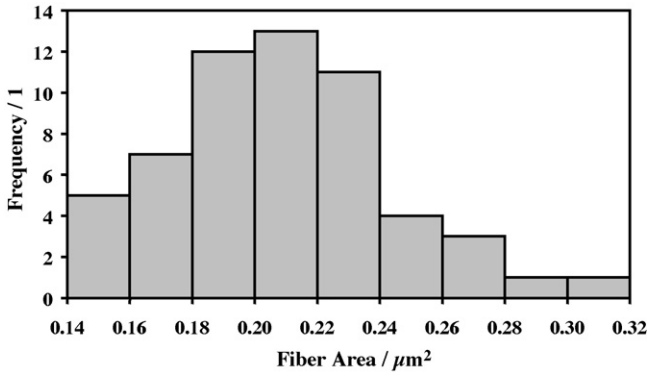

Fig. 3. Histogram of the cross-sectional areas of the copper fibres. Areas were calculated by converting this figure to a binary image and using MATLAB software to sum the pixels of the wires cross-sections.

of the wires cross-sections. The result of this analysis is shown in the histogram (Fig. 3) that classifies all wires between 0.14 and 0.32 μm^2 with an average at 0.21 μm^2. Approximating the wires' cross-sections as circles, the wire diameter would range from 420 to 640 nm with an average of 520 nm for a growth rate of 25 μm s^{-1}. The results are summarized in Table 1.

3.4. Comparison of the chemical reactivity

In previous studies the selective dissolution of either of the phases of a directionally solidified material was possible because of strong differences in their chemical behaviour [25–27]. In the present case, however, the chemistry of the two pure phases Cu and Ag is very similar. Both phases are pure elements in the copper group, the first sub group of the PSE.

Copper and silver are also known as coinage metals because, historically, their resistance to corrosion has made them suitable for producing coins. This resistance to corrosion can be attributed to their nobility. This results both, from the closed d-shell and the higher nuclear charge (compared to the period's alkali metal) which attracts the single valence s-electron. The d-shell does not adequately shield the valence s-electron, nor is there a second electron in the orbital as in the Zn group, so it requires considerable energy to remove the valence s-electron and corrode these metals. As expected, the nobility increases with increasing nuclear charge and is higher for silver with a standard potential of $E^{\circ}_{Ag/Ag^+} = +0.799$ V as compared to $E^{\circ}_{Cu/Cu^{2+}} = +0.337$ V. This difference in potential as well as the fact that a d-electron can be more easily employed as a valence electron in the case of copper (d^9-configuration) is the starting point for the electrochemical separation.

Table 1
Geometrical details of the different solidification batches

Growth rate, V (mm h^{-1})	Growth rate, V (μm s^{-1})	Fibre diameter, a (nm)	a^2V (m^3 s^{-1})
245	68.1	318	6.9×10^{-18}
91	25.0	526	6.9×10^{-18}
53	14.7	685	6.9×10^{-18}

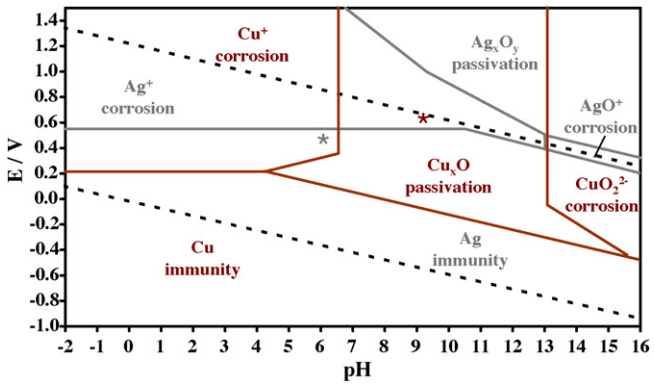

Fig. 4. Combined Pourbaix diagram for silver and copper. The grey asterisk indicates the electrochemical conditions used to produce silver nanopits. The brown asterisk indicates the conditions used to produce copper nanowires. The lines were calculated for a concentration of 10^{-5} mol l^{-1}. (For interpretation of the references to color in this figure legend, the reader is referred to the web version of the article.)

The combined Pourbaix diagram as shown in Fig. 4 is a superposition of the diagrams for copper and silver and was used as a guide for choosing conditions for electrochemical processing. Ignoring kinetics, Pourbaix calculated the domains of these diagrams using the Nernst equation and thermodynamic data [42], so the combined Pourbaix diagram served only as a starting point in the search for appropriate conditions. An idea of the cell's ideal behaviour can be obtained by applying the Nernst equation:

$$E = E^{\circ} + \frac{RT}{nF} \ln \frac{a_{ox}}{a_{red}} \quad (2)$$

in which E is the cell potential; E° the standard potential of the metal in question; R the ideal gas constant; T the temperature in Kelvin; n the number of electrons in the half-reaction; F the Faraday's constant, and a_{ox} and a_{red} are the activities of the oxidized and reduced species, respectively. For a solid metal the activity would be that of a pure phase, which is by definition 1. For very small nano-structures however, this value will approach more and more that of an alloy, or in this case the volume fraction of the metal [43].

3.5. Selective dissolution of copper

In the case of copper dissolution, with $E^{\circ}_{(Cu/Cu^{2+})} = +0.337$ V and $E^{\circ}_{(Cu/Cu^{2+})} = +0.500$ V, the activity of the oxidized species, Cu^{2+}, would be formally calculated to be 3.2×10^5 M. Such a concentration is impossible, but it suggests that the concentration of cupric ions would be thermodynamically driven to its maximum to ensure that the copper dissolution falls under kinetic control.

The greater nobility of silver made the selective dissolution of copper relatively straightforward. Selective dissolution of copper occurred in 1.0 M acetate buffer, pH 6.0, at 0.5 V (SHE). The dissolution is assumed to occur by the direct oxidation of the copper at a potential insufficient for oxidizing the silver. As the acetate salts of both metals are sufficiently soluble, no layers formed to coat the surfaces of the metals. Dissolution proceeded with the sky-blue tinting of the electrolyte characteristic of hydrated cupric cations (Figs. 5 and 6).

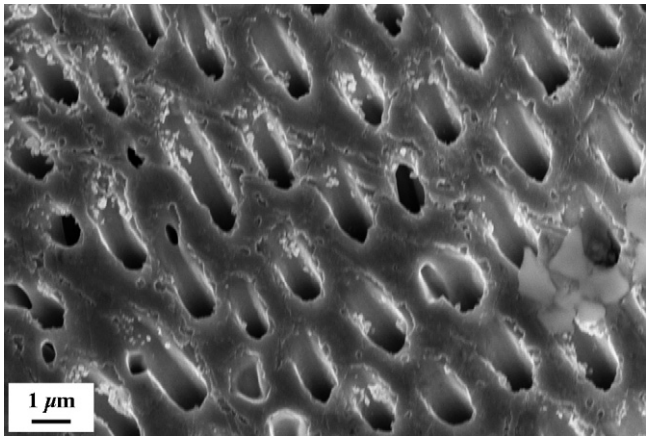

Fig. 5. SEM image of micropits in the silver matrix. The copper wires were dissolved electrochemically.

3.6. Selective dissolution of silver

Selective dissolution of the silver matrix occurred in 0.1 M borate buffer, pH 9.2, at 0.7 V (SHE), and was achieved through the passivation of the copper with oxide layers and the dissolution of the silver oxide formed concurrently. At anodic potentials in alkaline solution (pH 9.2) copper initially formed a layer of cuprous oxide, part of which then oxidized further to create a second layer of either cupric oxide or cupric hydroxide [44]. This bilayer effectively passivated the copper, preventing further oxidation and dissolution of the fibres. Meanwhile, a silver oxide was also formed but did not passivate the surface. During dissolution, a greyish-white substance precipitated from the sample, presumably argentous oxide. Samples were dissolved in steps totalling from 8 to 48 h. Dissolution of the silver matrix left protruding copper wires embedded in the sample. Diameters of the arrayed wires ranged from 300 nm (Fig. 7) to 650 nm (Fig. 8), with lengths of up to several microns. The length of the

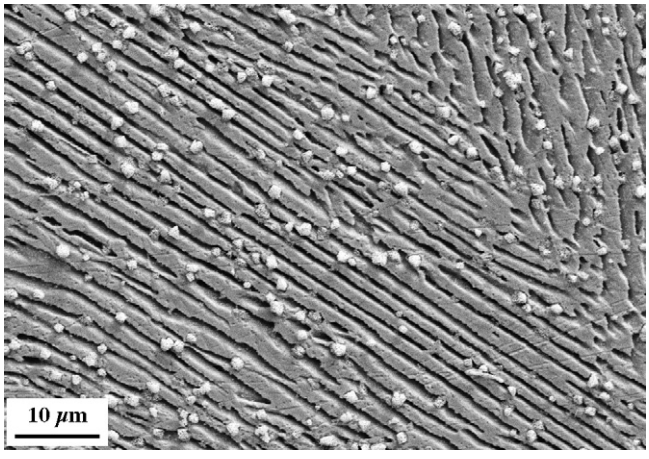

Fig. 6. SEM image of dissolved lamellar copper structures. The deposits on the sample could be removed by ultrasonification in pure water.

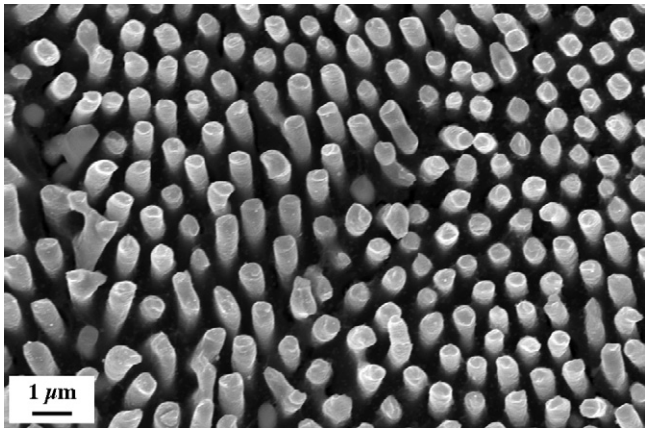

Fig. 7. Ordered copper wire array just beginning to be etched free from the silver matrix. The diameters of the wires are approximately 550 nm. The solidification speed was 25 $\mu m\,s^{-1}$.

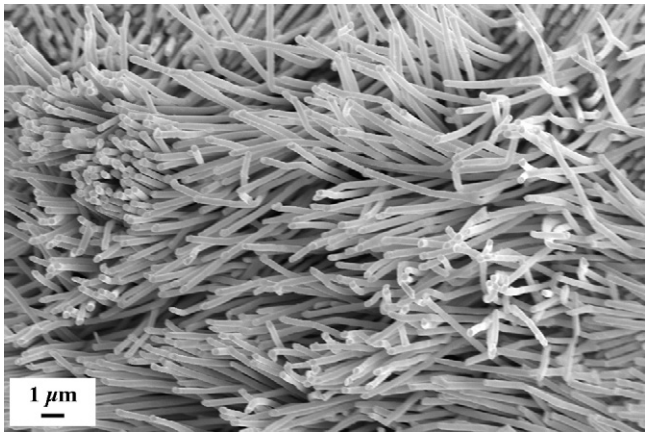

Fig. 8. Exposed copper wires after dissolution of the silver matrix for time segments totalling nearly 48 h. The wires have diameters of approximately 300 nm.

wires could be controlled by the dissolution time, with a longer time exposing longer wires from the matrix [45].

4. Conclusions

The results of this study demonstrate clearly, that the directional solidification of the silver copper eutectic leads to a nano-structured material consisting of Cu nanowires and lamellae in a silver matrix. This silver copper system with 31.8 vol.% Cu is a borderline case between lamellar systems with a symmetric composition and fibrous systems with asymmetric volume fractions. This is seen in the fact that copper forms both, lamellae and fibres in the same sample. For this system the crystallographic orientation relationship between the two solid phases will steer into either of both structures, depending on the corresponding structural undercooling and compositional undercooling. The important proportionality factor a^2V was quantitatively determined to be $6.9 \times 10^{-18}\,m^3\,s^{-1}$.

Favourable working points for the selective dissolution of either of the phases were derived from a combined Pourbaix diagram. Whereas the dissolution of the less noble copper wires for the production of a porous silver matrix was straightforward at pH 6.0 and 0.5 V (SHE) the route to dissolving silver selectively was less obvious. However, at pH 9.2 and 0.7 V (SHE) the driving force is sufficient for both metals to be oxidized, in case of copper the rate is sufficiently high to allow the copper to passivate while silver dissolves slowly.

Acknowledgements

The financial support of the Deutsche-Forschungs-Gemeinschaft for the project (HA3118/4-2) within the DFG Priority Programme 1165 “Nanowires and Nanotubes, from controlled Synthesis to Function” and a scholarship from the DAAD within the frame of the RISE program for SB are gratefully acknowledged.

References

[1] Y. Sakai, K. Inoue, H. Maeda, Acta Mater. 43 (1995) 1517.
[2] M. Motokawa, H. Nojiri, S. Mitsudo, Y. Inamura, IEEE Trans. Magn. 32 (1996) 2534.
[3] Y. Sakai, H.J. Schneider-Muntau, Acta Mater. 45 (1997) 1017.
[4] G. Frommeyer, G. Wassermann, Acta Metall. 23 (1975) 1353.
[5] Y. Sakai, K. Inoue, T. Asano, H. Wada, H. Maeda, Appl. Phys. Lett. 59 (1991) 2965.
[6] A. Bengalem, D.G. Morris, Acta Metall. Mater. 45 (1997) 397.
[7] Y. Sakai, H.J. Schneider-Muntau, Acta Metall. Mater. 45 (1997) 1017.
[8] S.I. Hong, M.A. Hill, Acta Metall. Mater. 46 (1998) 4111.
[9] S.I. Hong, M.A. Hill, Mater Sci. Eng. A 264 (1999) 151.
[10] H. Maeda, K. Inoue, T. Kiyoshi, T. Asano, Y. Sakai, T. Takeuchi, K. Itoh, H. Aoki, G. Kido, Physica B 216 (1996) 141.
[11] J.E. Crow, D.M. Parkin, H.J. Schneider-Muntau, N.S. Sullivan, Physica B 216 (1996) 146.
[12] M. von Ortenberg, O. Portugall, N. Puhlmann, H.U. Mueller, M. Barczewski, G. Machel, M. Thiede, Physica B 216 (1996) 158.
[13] S.I. Hong, M.A. Hill, Y. Sakai, J.T. Wood, J.D. Embury, Acta Metall. Mater. 43 (1995) 3313.
[14] S.I. Hong, M.A. Hill, Acta Mater. 46 (1998) 4111.
[15] M. Carrard, M. Gremaud, M. Zimmermann, W. Kurz, Acta Metall. Mater. 40 (1992) 983.
[16] D.J.S. Cooksey, A. Hellawell, J. Inst. Met. 95 (1967) 183.
[17] U. Hecht, L. Gránásy, T. Pusztai, B. Böttger, M. Apel, V.T. Witusiewicz, L. Ratke, J. De Wilde, L. Froyen, D. Camel, B. Drevet, G. Faivre, S.G. Fries, B. Legendre, S. Rex, Mater. Sci. Eng. R 46 (2004) 1.
[18] J. De Wilde, L. Froyen, S. Rex, Scripta Mater. 51 (2004) 533.
[19] J. De Wilde, L. Froyen, V.T. Witusiewicz, U. Hecht, J. Appl. Phys. 97 (2005) 113515.
[20] K. Suganuma, T. Murata, H. Noguchi, Y. Toyoda, J. Mater. Res. 15 (2000) 884.
[21] I. Shohji, T. Nakamura, F. Mori, S. Fujiuchi, Mater. Trans. 43 (2002) 1797.
[22] C.M.L. Wu, D.Q. Yu, C.M.T. Law, L. Wang, Mater. Sci. Eng. R 44 (2004) 1.
[23] M.N. Islam, A. Sharif, Y.C. Chan, J. Electron. Mater. 34 (2005) 143.
[24] G. Frommeyer, G. Wassermann, Phys. Stat. Sol. 27 (1975) 99.
[25] A.W. Hassel, B. Bello Rodriguez, S. Milenkovic, A. Schneider, Electrochim. Acta 50 (2005) 3033.
[26] A.W. Hassel, B. Bello Rodriguez, S. Milenkovic, A. Schneider, Electrochim. Acta 51 (2005) 795.
[27] A.W. Hassel, A.J. Smith, S. Milenkovic, Electrochim. Acta 52 (2006) 1799.
[28] S. Milenkovic, A. Schneider, A.W. Hassel, Gold Bull. 39 (2006) 185.
[29] S. Milenkovic, A. Schneider, A.W. Hassel, Nano Lett. 6 (2006) 794.
[30] W.C. Roberts-Austen, Proc. Roy. Soc. Lond. 23 (1875) 481.
[31] W.C. Roberts-Austen, Engineering 52 (1891) 579.

[32] C.T. Heycock, F.H. Neville, Philos. Trans. Roy. Soc. (London) A189 (1897) 25.
[33] K. Friedrich, A. Leroux, Metallurgie 4 (1903) 293.
[34] W.F. Roesner, U.S. Bur. Std. J. Res. 3 (1929) 343.
[35] D. Stockdale, J. Inst. Met. 43 (1930) 193.
[36] H. Moser, J. Otto, W. Thomas, Z. Phys. 175 (1963) 327.
[37] M. Hansen, K. Anderko, Constitution of Binary Alloys, Originally Published by McGraw-Hill, Reprinted and Available from Genium Publishing, Schenectady, NY, USA, 1958.
[38] M. Hansen, R.P. Elliot, Bull. Alloy Phase Diagrams 1 (1980) 41.
[39] W. Broniewski, S. Kotacz, Compt. Rend. 194 (1932) 973.
[40] J.D. Hunt, K.A. Jackson, Trans. Met. Soc. AIME 236 (1966) 843.
[41] J.D. Hunt, J.P. Chilton, J. Inst. Met. 91 (1962) 338.
[42] M. Pourbaix, Atlas of Electrochemical Equilibria in Aqueous Solutions, National Association of Corrosion Engineers, Houston, 1974.
[43] J. Erlebacher, M.J. Aziz, A. Karma, N. Dimitrov, K. Sieradzki, Nature 410 (2001) 450.
[44] H.-H. Strehblow, B. Titze, Electrochim. Acta 25 (1979) 839.
[45] A.W. Hassel, S. Milenkovic, U. Schürmann, H. Greve, V. Zaporojtchenko, R. Adelung, F. Faupel, Langmuir 23 (2007) 2091.